SUPPORTING INFORMATION

Kinetic stabilization of *N*,*N*-dimethyl-2-propyn-1-amine *N*-oxide by encapsulation

Albano Galán[‡], Guzmán Gil-Ramirez[‡] and Pablo Ballester[*,‡,§]

‡ *Institute of Chemical Research of Catalonia (ICIQ), Avgda. Països Catalans, 16, 43007, Tarragona, Spain.*

§ *Catalan Institution for Research and Advanced Studies (ICREA), Passeig Lluís Companys, 23, 08018, Barcelona, Spain.*

pballester@iciq.es

Table of Contents

EXPERIMENTAL SECTION

Tetranitro calix[4]pyrrole **5**[1], bis[2]catenane **6**[2], octamethylcalix[4]pyrrole **9**[3] and dinitrocalix[4]pyrrole **8**[4] were synthesized according to reported procedures.

SYNTHESIS of DIMETHYL PROP-2-YNYL AMINE *N*-OXIDE **1a**

A solution of 2.40 mmol (0.59 g) of m-chloroperbenzoic acid in chloroform was added gradually at 0-5ºC to an ice-cooled, stirred solution of 2.40 mmol (0.26 mL) of the amine in chloroform. Stirring was continued for a total of 3 hours, during which the mixture was allowed to come to room temperature. The solution was passed through a column of alkaline alumina (100-200 mesh, ca. 30 times the weight of the combined starting materials), and traces of unreacted amine were removed by washing with chloroform. Posterior elution with methanol-chloroform (5/95) gave the amine N-oxide in 80 % yield, as an off-white solid. The solid rapidly (several hours) decomposes at room temperature. ^{1}H NMR (CD_2Cl_2, 500 MHz, 298K) δ (ppm): 4.06 (d, 2H, J=2.59 Hz), 3.28 (s, 6H), 2.75 (t, 1H, J=2.59 Hz).[5]

---

[1] Gil-Ramirez, G.; Escudero-Adan, E. C.; Benet-Buchholz, J.; Ballester, P., *Angew. Chem., Int. Ed.*, **2008**, *47*, 4114-4118.
[2] Chas, M.; Ballester, P., *Chem. Sci.*, **2012**, *3*, 186-191.
[3] Sessler, J. L.; Gross, D. E.; Cho, W. S.; Lynch, V. M.; Schmidtchen, F. P.; Bates, G. W.; Light, M. E.; Gale, P. A., *J. Am. Chem. Soc.*, **2006**, *128*, 12281-12288.
[4] Cafeo, G.; De Rosa, M.; Kohnke, F. H.; Neri, P.; Soriente, A.; Valenti, L., *Tetrahedron Lett.*, **2008**, *49*, 153-155.
[5] Khuthier, A. H.; Aliraqi, M. A.; Hallstrom, G.; Lindeke, B., *J. Chem. Soc., Chem. Commun.*, **1979**, 9-10.

SYNTHESIS of DIMETHYL PROPYL AMINE N-OXIDE **7**

A solution of 12.62 mmol (1.1 g) of dimethylpropylamine in 3 mL of methanol is heated for three hours at 90 ºC in a sealed tube in the presence of 25.2 mmol (0.8 mL) of hydrogen peroxide. The cooled crude reaction mixture is passed through a basic alumina column eluting first with chloroform and finally with chloroform:methanol 95:5 to elute the desired product as a white solid that was dried overnight under high vacuum. ^{1}H NMR (CD_2Cl_2, 500 MHz, 298K) δ (ppm): 3.17 (m, 2H), 3.12 (s, 6H), 1.89 (m, 2H), 1.01 (t, 3H, d=7.36 Hz).[6]

[6] Volz, H.; Gartner, H. *Eur. J. Org. Chem.* **2007**, 2791-2801.

NMR EXPERIMENTS

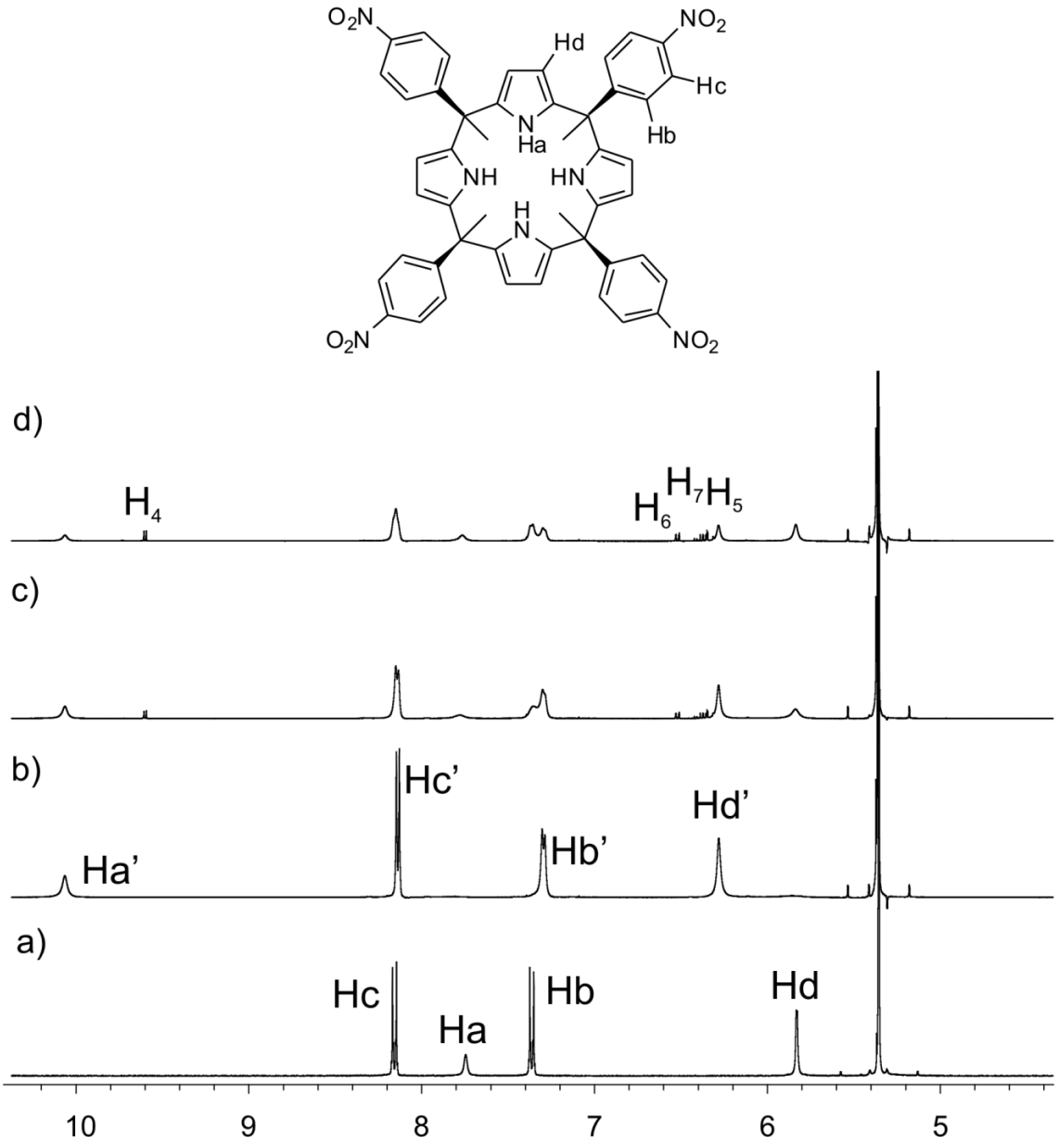

Figure S1. Selected regions of ^{1}H NMR spectra (298 K, 500 MHz) of: a) Calixpyrrole **5** in CD_2Cl_2; b) a 2.6 mM solution of **1a** in the presence of 1 eq. of **5** in CD_2Cl_2 after 0 hours; c) after 25 hours; and d) after 60 hours. Primed letters indicate signals of proton in the bound receptor. As the decomposition of **1a** to **3** progresses, included **1a** must be released to the bulk solution to maintain the equilibrium **1a** + **5** ↔ .**1a**⊂**5.** This process produces the appearance of a new set of signals in the ^{1}H NMR spectra (c,d) for some of the protons of

free **5** i.e. Ha and Ha'. Free and bound **5** are said to be involved in a slow chemical exchange process on the ^{1}H NMR timescale. Because the proton signals for the aromatic proton Hc and Hc' have similar chemical shifts for the free and the bound calix they show intermediate exchange.

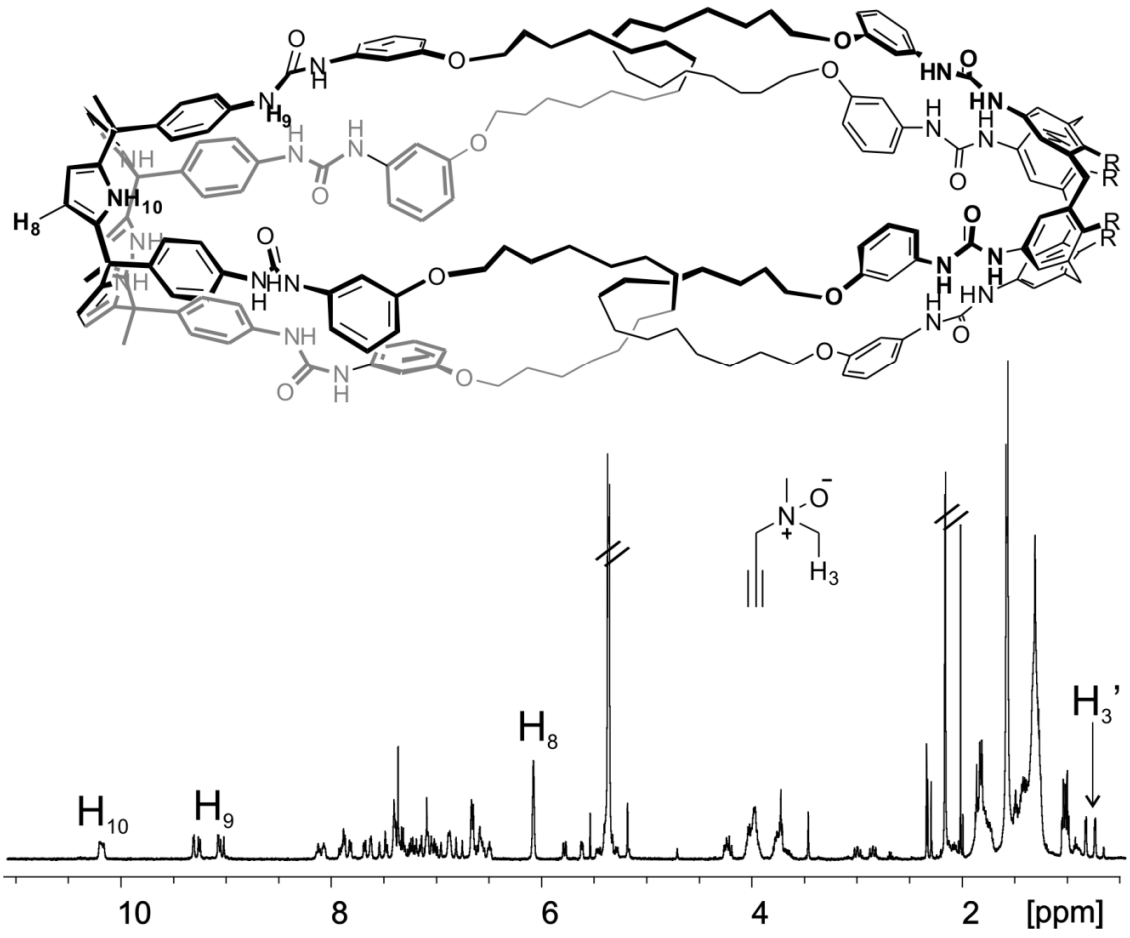

Figure S2. a) ^{1}H NMR spectrum of a CD_2Cl_2 solution containing an equimolar mixture of *N*-oxide **1a** and biscatenane **6** (0.5 mM).

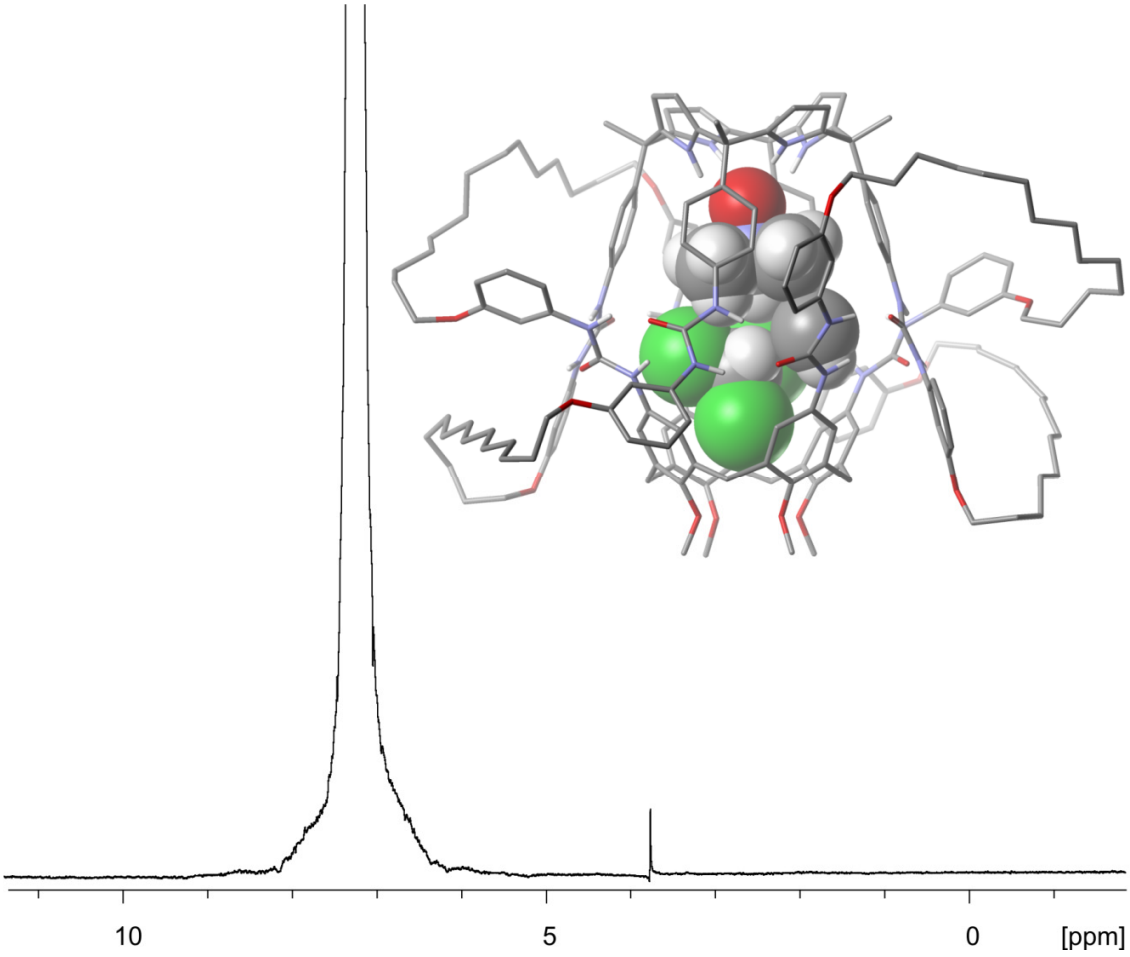

Figure S3. GOESY ^{1}H NMR spectrum of a $CHCl_3$ solution containing an equimolar mixture of *N*-oxide **1a** and biscatenane **6**. The signal of the proton corresponding to the co-included molecule of chloroform appears at 3.78 ppm. Inset: energy minimized structure of the container **6** with the *N*-oxide **1a** included in the cavity and one molecule of chloroform co-íncluded. Both **1a** and chloroform are showed as CPK models. For clarity non-polar hydrogen atoms have been removed in the container that is shown in stick representation.

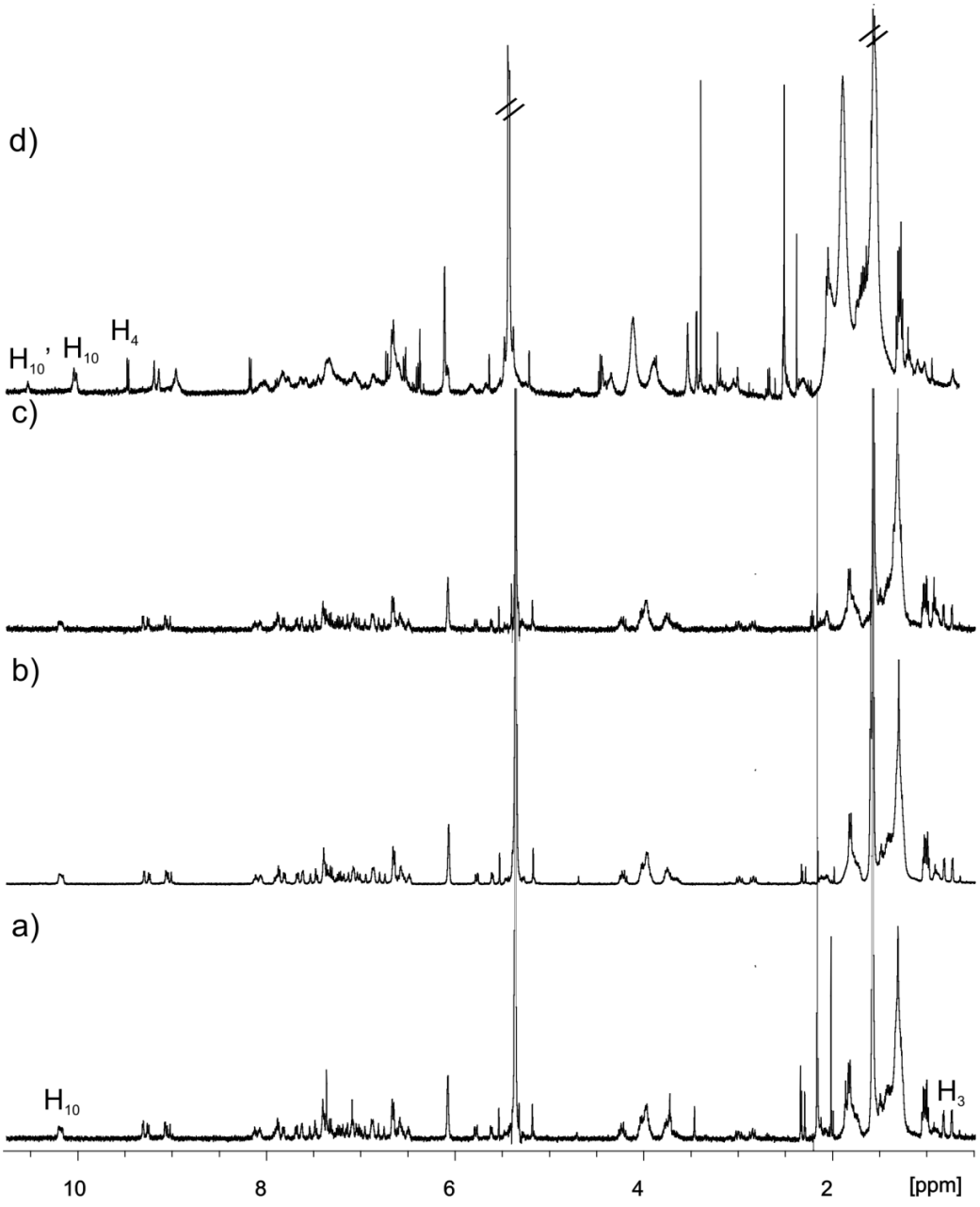

Figure S4 ^{1}H NMR spectra of CD_2Cl_2 solutions containing an equimolar mixture of *N*-oxide **1a** and biscatenane **6** (0.5 mM) after: a) 0 hours; b) 1 week, and c) 2 months; d) three hours after the addition of 10 equivalents of a competitive guest 4-dimethylamino pyridine *N*-oxide (DMAP-NO) to the previous sample (c). The formation of the inclusion complex DMAP-NO⊂**6** is evidenced by the emergence of a new signal corresponding to the pyrrolic NH protons, H_{10}'. Thus, **1a** is partially removed from the cavity of **6** and rapidly

experiences the decomposition in the bulk solution affording propenal, which is detected by observation of the signals of the aldehyde proton H_4.

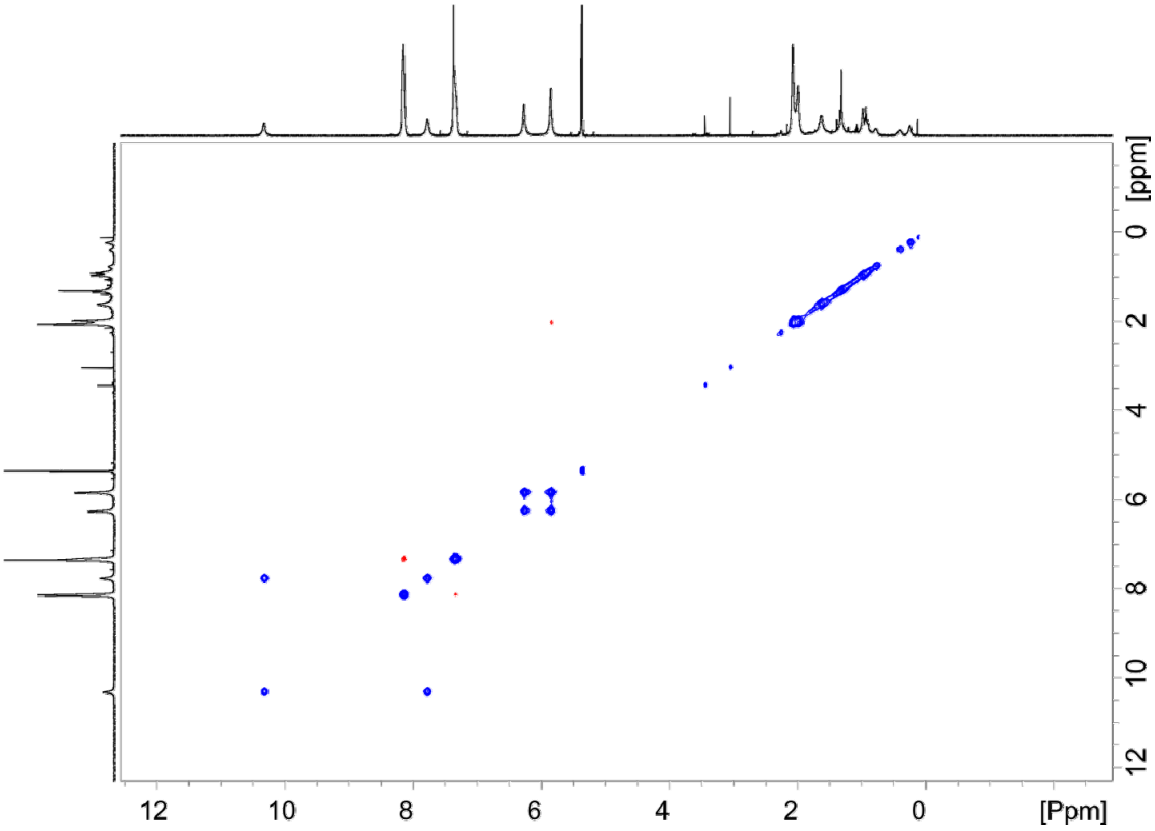

Figure S5. EXSY ^{1}H NMR spectrum of a d_2-dichloromethane solution containing a 2:1 mixture of tetranitrocalixpyrrole **5** and *N*,*N*-dimethyl-*N*-propyl amine *N*-oxide **7**. The observation of separate protons signals for the β-pyrrolic and NH protons of free and bound **5** indicates that they are involved in a chemical exchange process that is slow on the ^{1}H NMR timescale. This fact is also evidenced by the existence of cross-peaks between those signals. The sign of the cross peaks must be the same than the diagonal peaks if they are due to chemical exchange. Integration of diagonal and cross peaks allowed the calculation of the rate constant values for the spin exchange process.

FITS OF THE KINETIC DATA AND SIMULATED SPECIATION DIAGRAMS

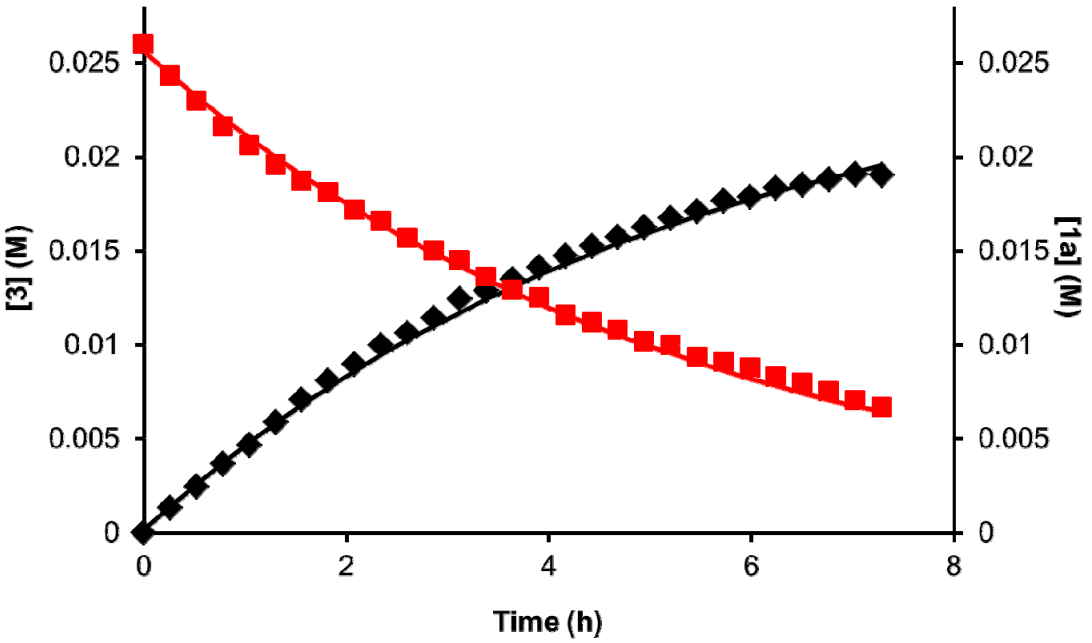

Figure S6. Kinetic data for the decomposition of **1a** (red squares) ($[\mathbf{1a}]_0$ = 26 mM) free in CD_2Cl_2 solution and the formation of **3** (black diamonds). The lines represent the best fit of the data using differential kinetics as implement in SPECFIT to the model:

$$\mathbf{1a} \xrightarrow{k_1} \mathbf{3}$$

$[1a]_o = 26$ mM $\qquad k_1 = 5.3 \times 10^{-5} \pm 0.3 \times 10^{-5}\ s^{-1}$

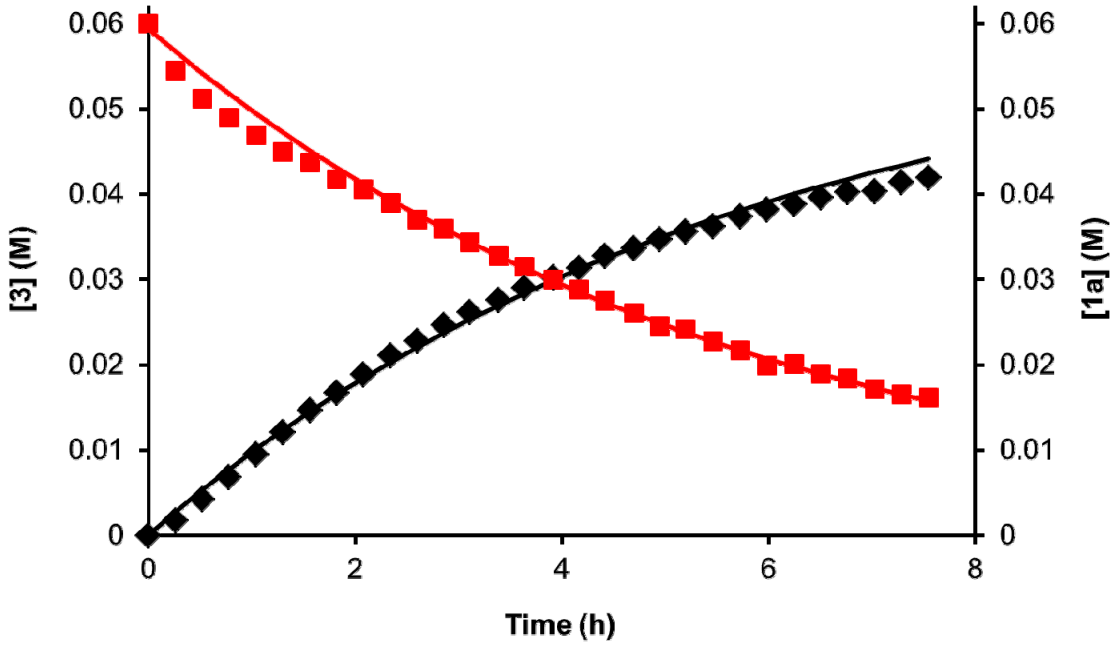

Figure S7. Kinetic data for the decomposition of **1a** (red squares) ($[\mathbf{1a}]_0$ = 60 mM) free in CD_2Cl_2 solution and the formation of **3** (black diamonds). The lines represent the best fit of the data using differential kinetics as implement in SPECFIT to the model:

$$\mathbf{1a} \xrightarrow{k_1} \mathbf{3}$$

$[1a]_o = 60$ mM $\qquad k_1 = 4.9 \times 10^{-5} \pm 0.4 \times 10^{-5}\ s^{-1}$

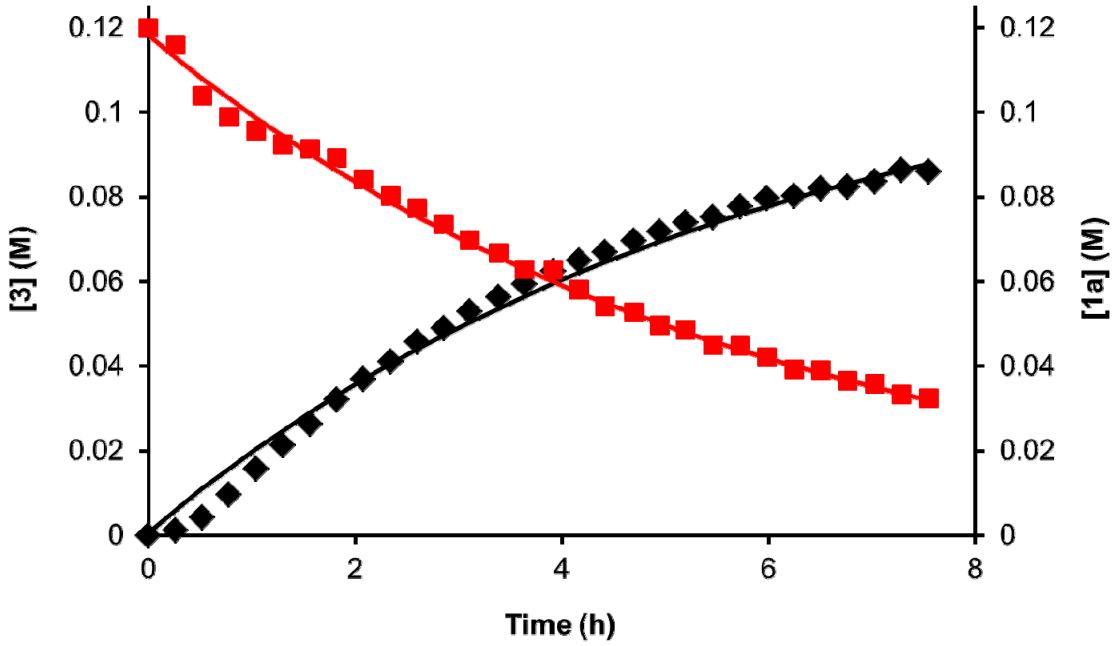

Figure S8. Kinetic data for the decomposition of **1a** (red squares) ($[\mathbf{1a}]_0$ = 120 mM) free in CD_2Cl_2 solution and the formation of **3** (black diamonds). The lines represent the best fit of the data using differential kinetics as implement in SPECFIT to the model:

$$\mathbf{1a} \xrightarrow{k_1} \mathbf{3}$$

$[1a]_o$ = 120 mM $k_1 = 4.8 \times 10^{-5} \pm 0.4 \times 10^{-5}\ s^{-1}$

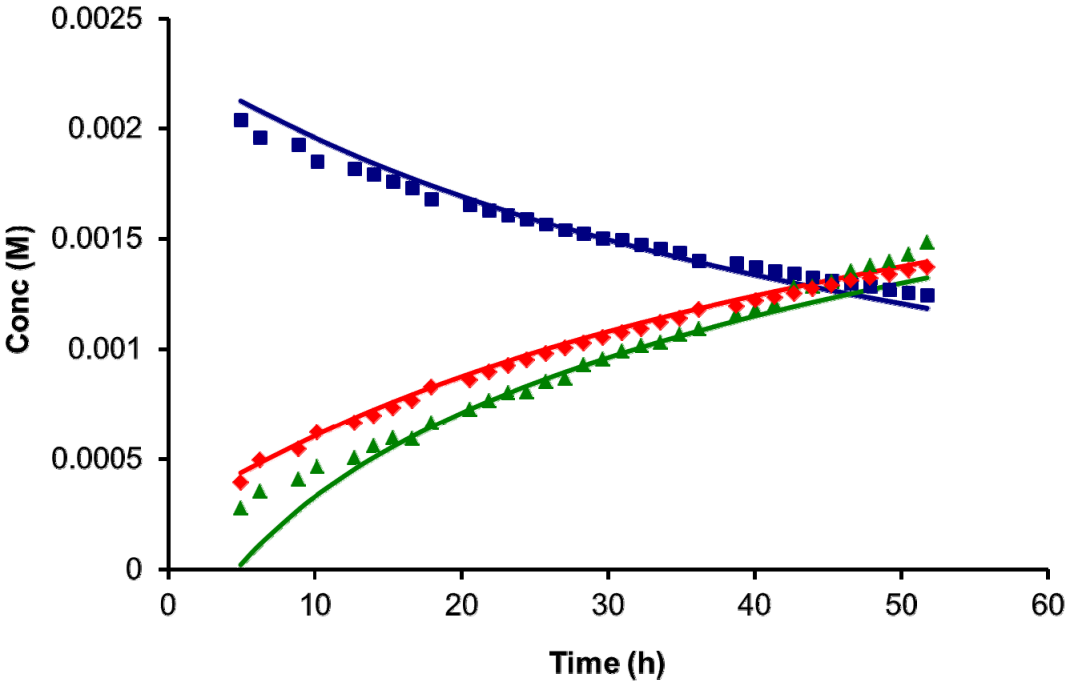

Figure S9. Data points corresponding to the concentration changes experienced by the different species present in solution during the decomposition reaction of **1a** ($[\mathbf{1a}]_0$ = 2.5 mM) to propenal **3** in the presence of 1 equivalent of tetranitro calixpyrrole **5**: **1a⊂5** (blue squares), **5** (red diamonds) and **3** (green triangles) The lines represent the best fit of the experimental data using the differential kinetics module of SPECFIT to the model depicted below:

$$\mathbf{1a} \xrightarrow{k_1} \mathbf{3}$$

$$\mathbf{1a} + \mathbf{5} \underset{k_{off}}{\overset{k_{on}}{\rightleftharpoons}} \mathbf{1a{\subset}5}$$

The first half-life for the decomposition of **1a** in the presence of calixpyrrole **5** is estimated by visual extrapolation as > 50 hours. The fit returned the value of $k_{on} = 1.2 \times 10^4$ M^{-1} s^{-1} as the only variable to refine.

In all kinetic experiments described above the values of the concentration for the different species were calculated by ^{1}H NMR integration of selected proton signals of each species.

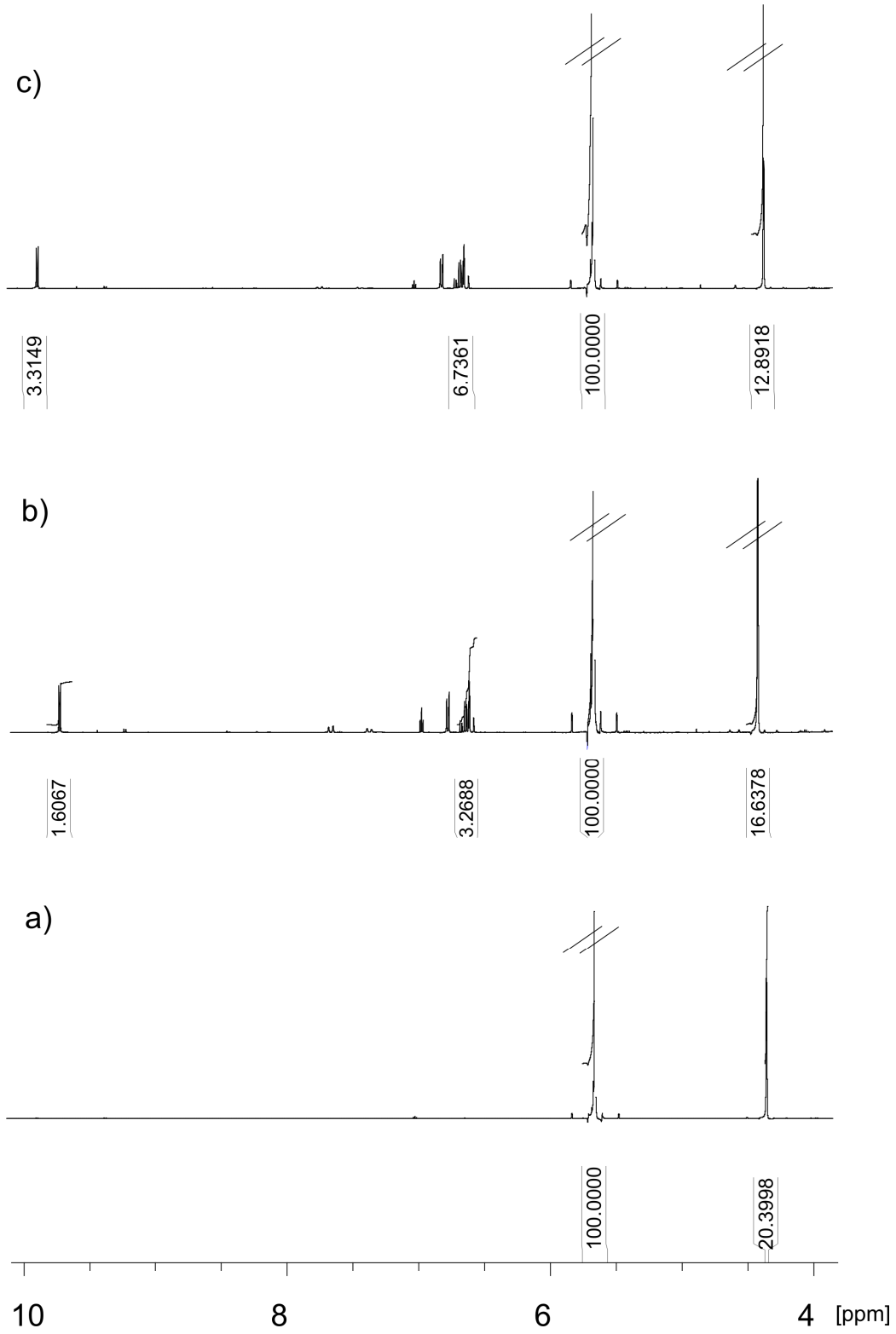

Figure S10. ^{1}H NMR and integral values of a 26 mM CD_2Cl_2 of *N*-oxide **1a** after a) 0 min b) 75 min c) 150 min. The baseline was automatically corrected before integration.

The area of the integral for the residual peak of the non-deuterated methylene chloride solvent was used as reference to normalize the areas of the signals of the protons of the substrate **1a** and product **3**.

At t = 0 the normalized area of the integral for the signal of the methylene protons of the *N*-oxide **1a** is proportional to the initial concentration (26 mM); c = $[\mathbf{1a}]_o$/area =2.55. The proportionally constant calculated at t = 0 was used to derive the concentration of *N*-oxide 1a at different times using the formula $[\mathbf{1a}]_t = \text{area}_t \times c$.

A similar procedure was used for the calculation of the concentrations of the other species with time.

$$[\mathbf{1a}]_{t=0} = 26 \text{ mM}; [\mathbf{1a}]_{t=75 \text{ min}} = 21.2 \text{ mM}; [\mathbf{1a}]_{t=150 \text{ min}} = 16.4 \text{ mM}$$

$$[\mathbf{3}]_{t=0} = 0 \text{ mM}; [\mathbf{3}]_{t=75 \text{ min}} = 4.17 \text{ mM}; [\mathbf{3}]_{t=150 \text{ min}} = 8.59 \text{ mM}$$

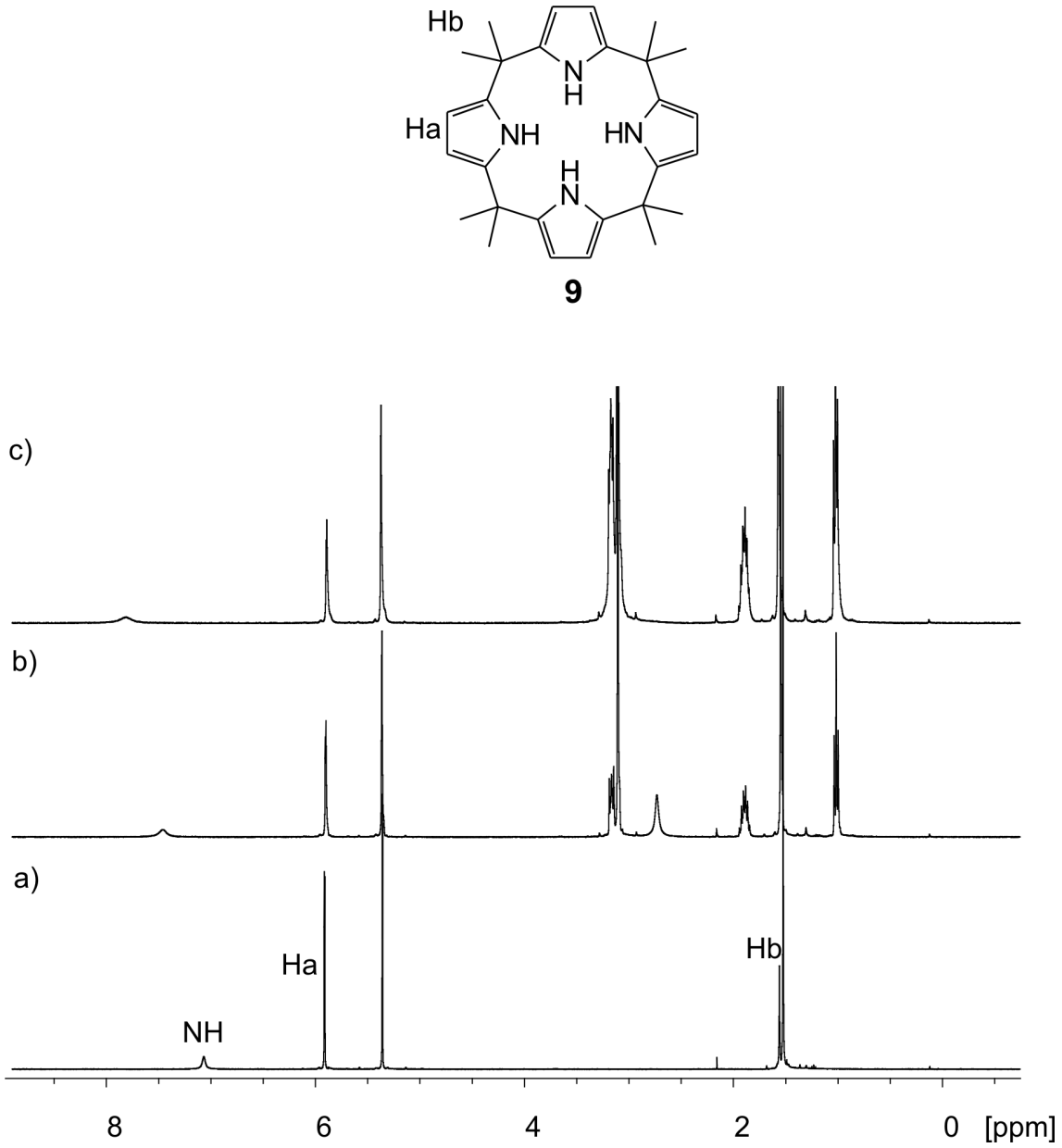

Figure S11. ^{1}H NMR spectra of a CD_2Cl_2 solution of octamethyl calixpyrrole **9** containing a) 0 eq. of *N*-oxide **7** b) 5 eq. of **7** c) 10 eq. of **7**

The host guest complexation process shows fast exchange in the NMR timescale.

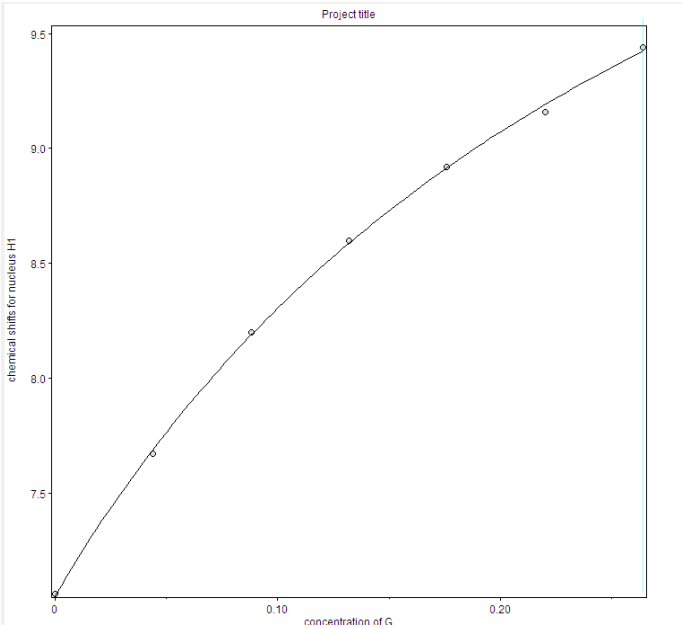

Figure S12. Fit of the data for the chemical changes of the NH protons in the titration of octamethyl calix[4]pyrrole **9** calix[4]pyrrole with *N*-oxide **7**

The data was fit to a theoretical 1:1 binding model. The theoretical curve corresponds to an association constant lower than 10 M^{-1} . δ_{NH}(**7**⊂**9**) = 12.22 ppm extrapolated at 100% bound using HypNMR software.

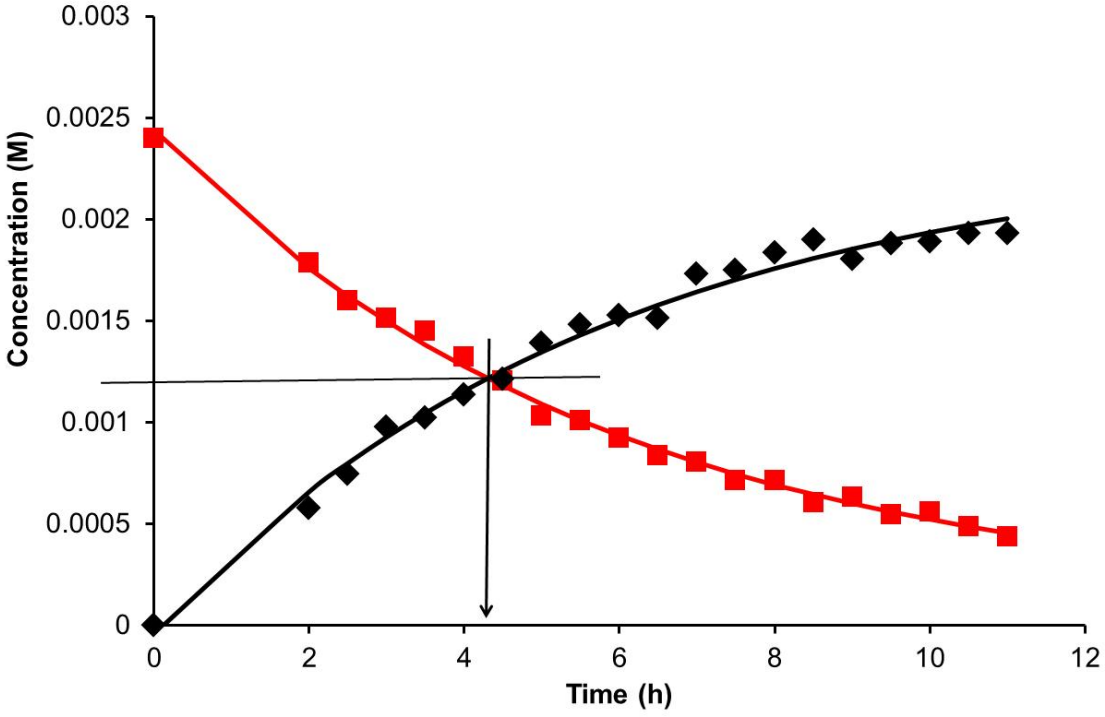

Figure S13. Kinetic data for the decomposition of **1a** (red squares) ([**1a**]$_0$ = 2.4 mM) in CD_2Cl_2 solution and the formation of **3** (black diamonds) in the presence of 1 equivalent of octamethyl calixpyrrole **9.** The lines represent the best fit of the data using differential kinetics as implement in SPECFIT to the model:

$$\mathbf{1a} \xrightarrow{k_1} \mathbf{3}$$

$[1a]_o = 2.4$ mM $\qquad k_1 = 4.8 \times 10^{-5} \pm 0.2 \times 10^{-5}\ s^{-1}$

The value of the rate constant k_1 for the decomposition is very close to the one determined for free **1a** in bulk solution. The association constant for the complex between the octamethylcalixpyrrole **9** and the *N*-oxide is < 10 M^{-1}.

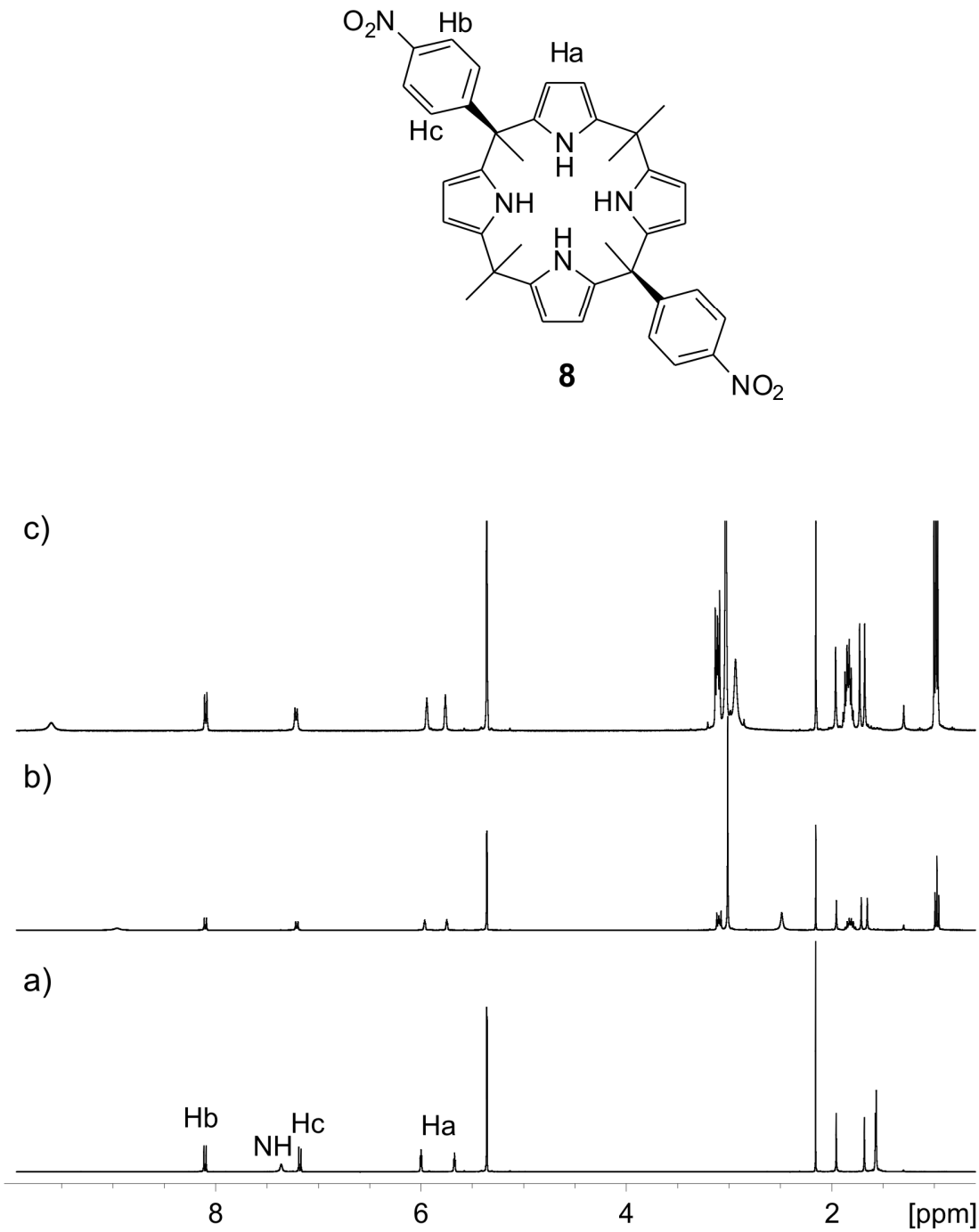

Figure S14. ^{1}H NMR spectra of a CD_2Cl_2 solution of dinitro calixpyrrole **8** containing a) 0 eq. of *N*-oxide **7** b) 5 eq. of **7** c) 10 eq. of **7**

The host guest complexation process shows fast exchange in the NMR timescale.

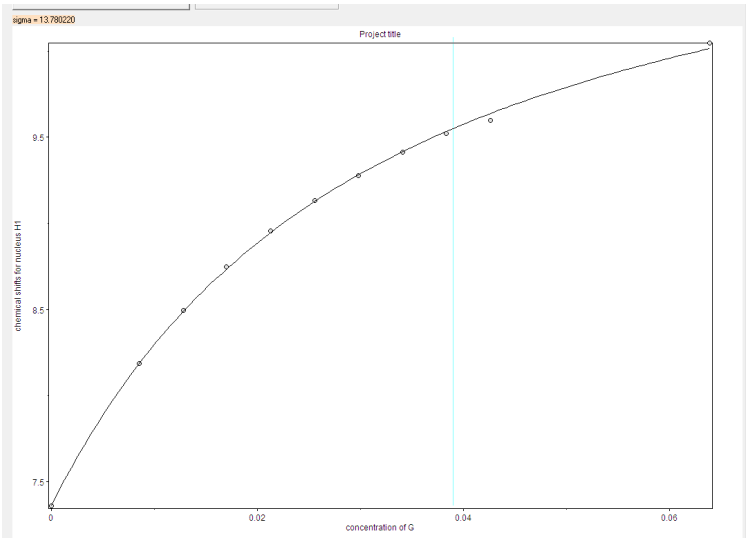

Figure S15. Fit of the data for the chemical shift changes of the NH protons in the titration of dinitro calix[4]pyrrole **8** with *N*-oxide **7** to a 1:1 binding model. The theoretical curve corresponds to an association constant value of K (**7**⊂**8**) = 35 M^{-1} ; δ_{NH}(**7**⊂**8**) = 11.25 ppm extrapolated at 100% bound using HypNMR software.

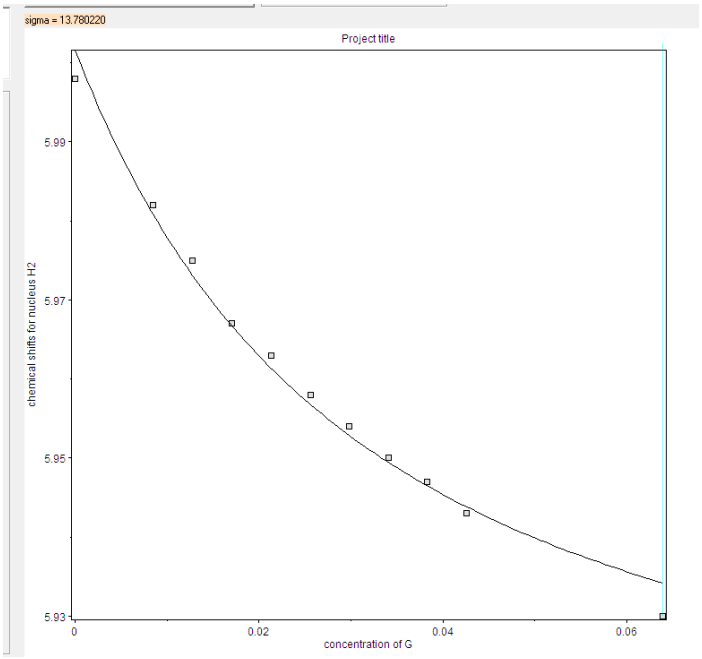

Figure S16. Fit of the data for the chemical shift changes of the beta pyrrole protons Ha in the titration of a CD_2Cl_2 solution of dinitro calix[4]pyrrole **8** with *N*-oxide **7** to a 1:1 binding model. The theoretical curve corresponds to an association constant value of K (**7**⊂**8**) = 35 M^{-1} . δ_{Ha}(**7**⊂8) = 5.91 ppm extrapolated at 100% bound using HypNMR software

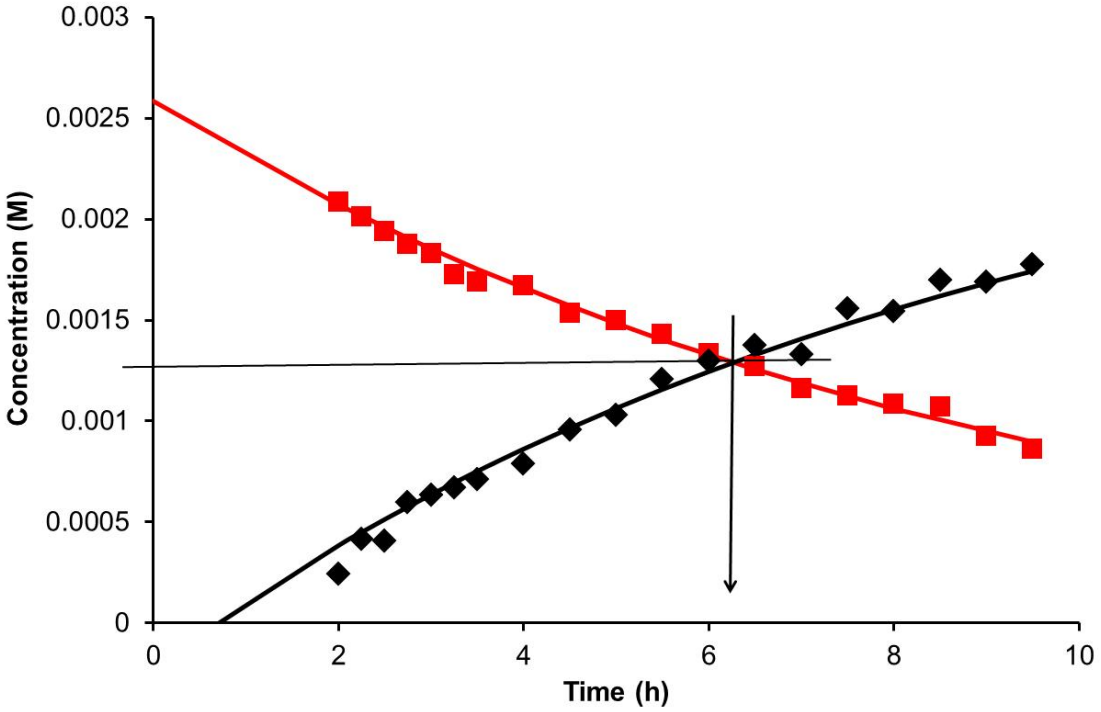

Figure S17. Kinetic data for the decomposition of **1a** (red squares) ([**1a**]$_0$ = 2.7 mM) and the formation of **3** (black diamonds) in CD_2Cl_2 solution in the presence of 1 equivalent of dinitro calixpyrrole **8**. The lines represent the best fit of the data using differential kinetics as implement in SPECFIT to the model:

$$\mathbf{1a} \xrightarrow{k_1} \mathbf{3}$$

$[1a]_o = 2.7$ mM $\qquad k_1 = 3.0 \times 10^{-5} \pm 0.3 \times 10^{-5}\ s^{-1}$

The calculated value for k_1 represents a negligible increment of the kinetic stabilization of the *N*-oxide **1a** provided by 8. The association constant for the complex between dinitrocalix[4]pyrrole **8** and *N*-oxide **7** is 35 M^{-1}.

The fact that calixpyrroles **8** and **9** do not stabilize kinetically the decomposition **1a** supports the fact that the kinetic stabilization of the *N*-oxide is a consequence of the formation of highly thermodynamically stable complexes by encapsulation in containers **5** and **6**.

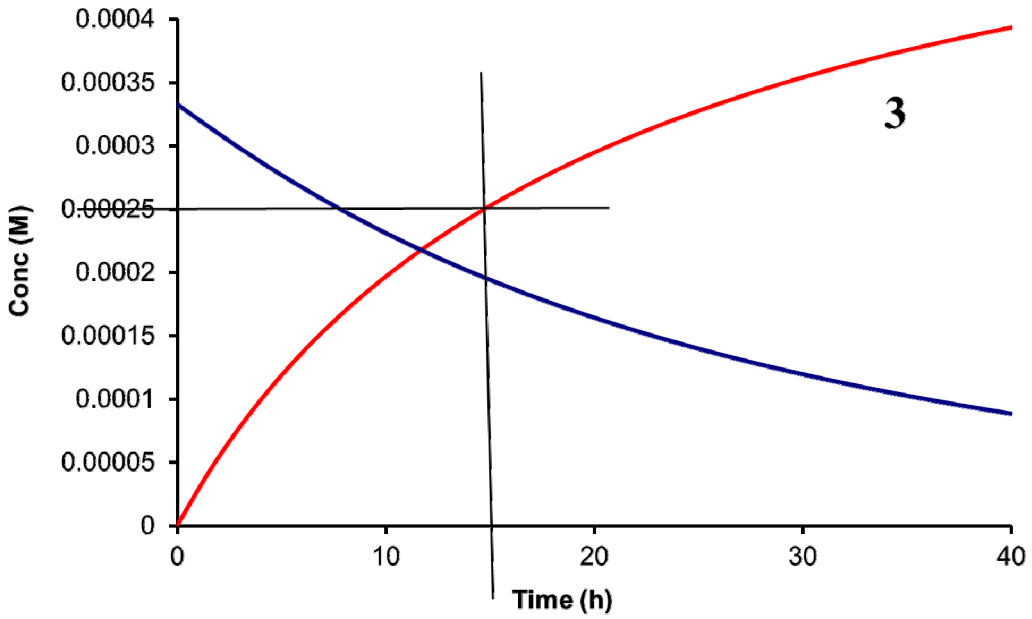

Figure S18. Simulated speciation diagram obtained for the decomposition of a solution of *N*-oxide **1a** ($[\mathbf{1a}]_0$ = 0.5 mM) in the presence of 1 equivalent of calixpyrrole **5**. The first half-life estimated by curve interpolation is 15 hours. Red line represents the formation of acrolein **3** and the blue line the disappearance of the **1a⊂5** complex. The concentrations of **1a** and **5** free are omitted for clarity. This simulation serves to demonstrate that the value of the first half-live of **1a** is dependent of its initial concentration when the decomposition obeys the following kinetic model

$$\mathbf{1a} \xrightarrow{k_1} \mathbf{3}$$

$$\mathbf{1a} + \mathbf{5} \underset{k_{off}}{\overset{k_{on}}{\rightleftharpoons}} \mathbf{1a{\subset}5}$$

On the contrary, the half-life value of **1a** free in solution is independent of its initial concentration because it follows a first order decomposition rate law (see Figures S6-S8).

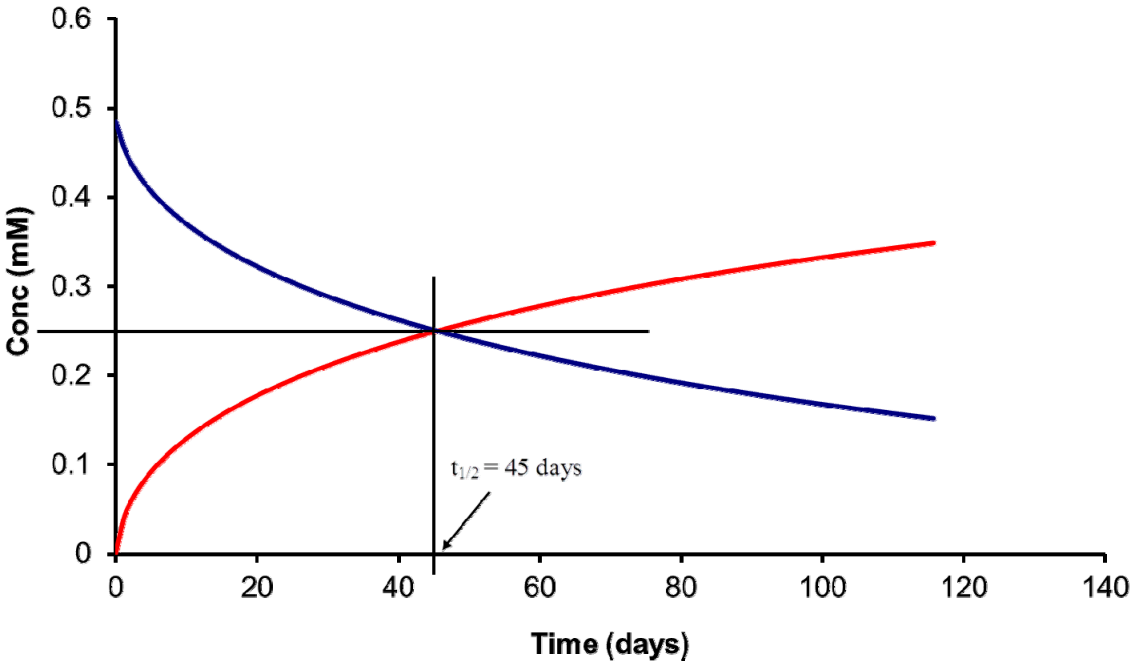

Figure S19. Speciation diagram obtained for the simulation of the decomposition of a solution of *N*-oxide **1a** (0.5 mM) in the presence of a putative molecular container producing a 1:1 encapsulation complex with a stability constant $K = k_{on}/k_{off} = 2 \times 10^6\ M^{-1}$. The first half-life, estimated by curve interpolation, is 45 days. Red line represents the formation of acrolein **3** and the blue line the disappearance of the putative encapsulation complex of **1a**.

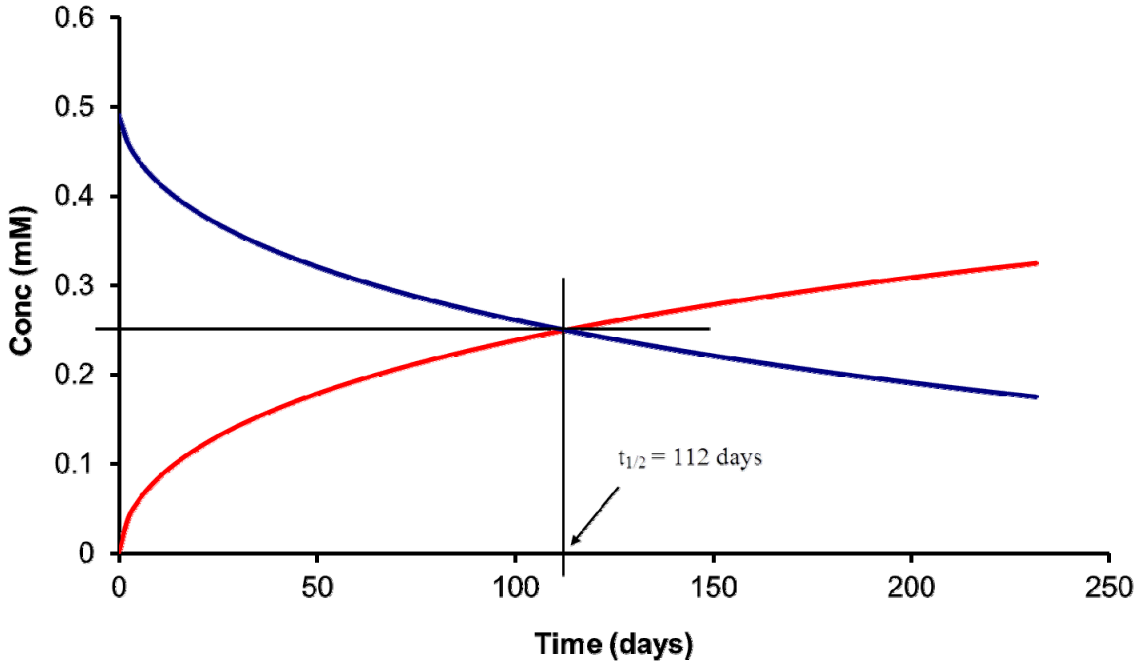

Figure S20. Speciation diagram obtained for the simulation of the decomposition of a solution of *N*-oxide **1a** (0.5 mM) in the presence of a putative molecular container producing a 1:1 encapsulation complex with a stability constant $K = k_{on}/k_{off} = 5 \times 10^6$ M^{-1}. The apparent first half-life estimated by curve interpolation is 112 days. Red line represents the formation of acrolein **3** and the blue line the disappearance of the putative encapsulation complex **1a**. It is worthy to note, the dramatic increase in the value of the first half-life that is predicted by the simulation upon subtle variations of the stability constant of the encapsulation complex. A 2.5 fold increase in *K* represents a change of 67 days in the first half-life of **1a**.

ITC EXPERIMENTS

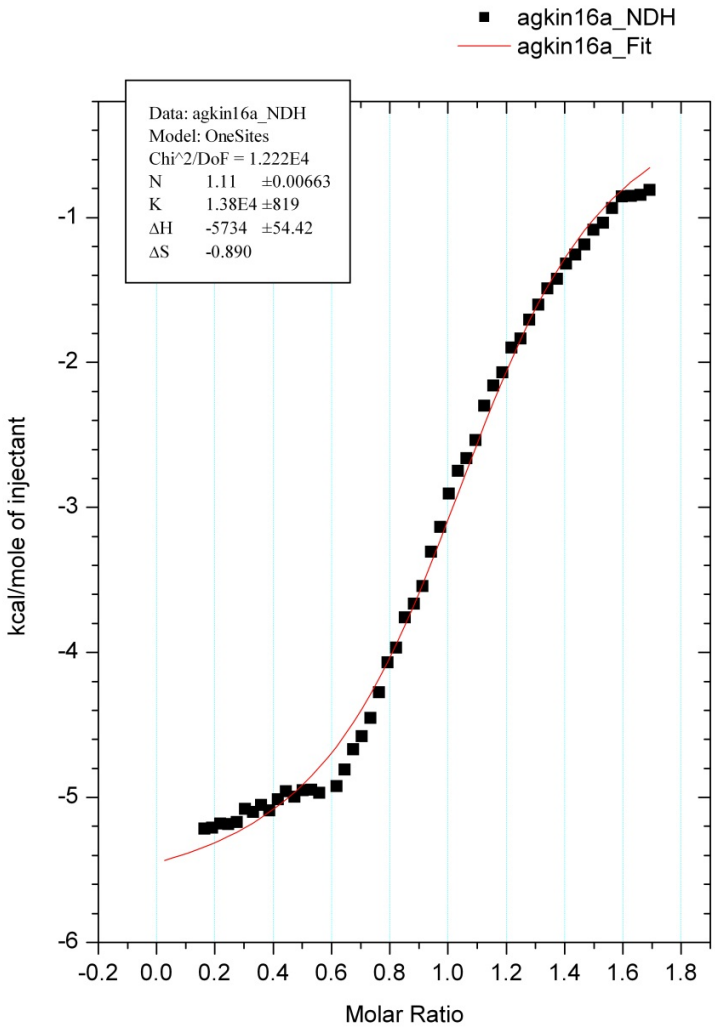

Figure S21. Normalized integration heat *vs* molar ration obtained in the ITC experiment of a CH_2Cl_2 solution of calixpyrrole **5** with *N*-oxide **7**. Fit to the theoretical binding isotherm (red line) using a 1:1 binding model. The mathematical analysis of the titration data was performed using the Origin software.

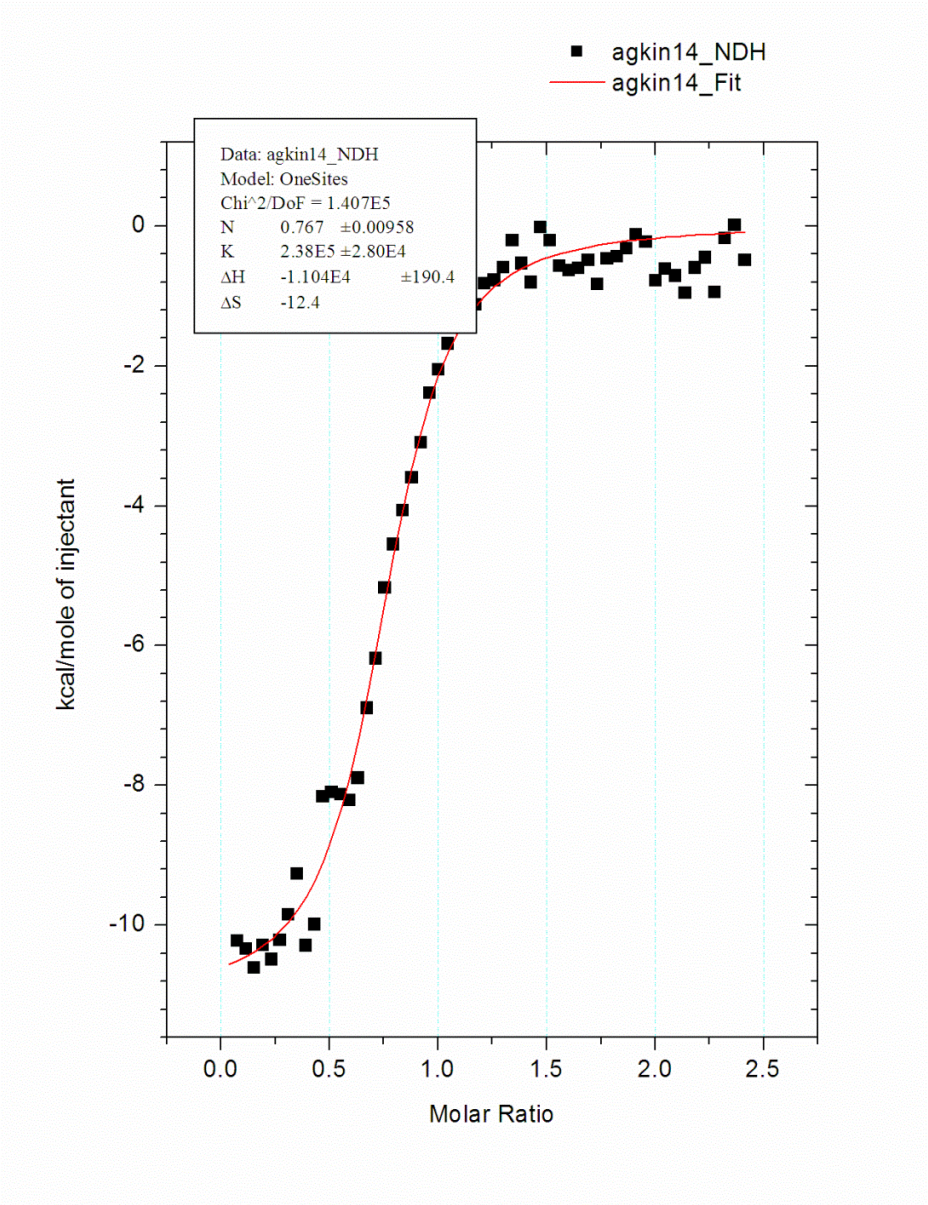

Figure S22. Normalized integration heat *vs* molar ration obtained in the ITC experiment of a $CHCl_3$ solution of biscatenane **6** with *N*-oxide **7**. Fit to the theoretical binding isotherm (red line) using a 1:1 binding model. The mathematical analysis of the titration data was performed using the Origin software.

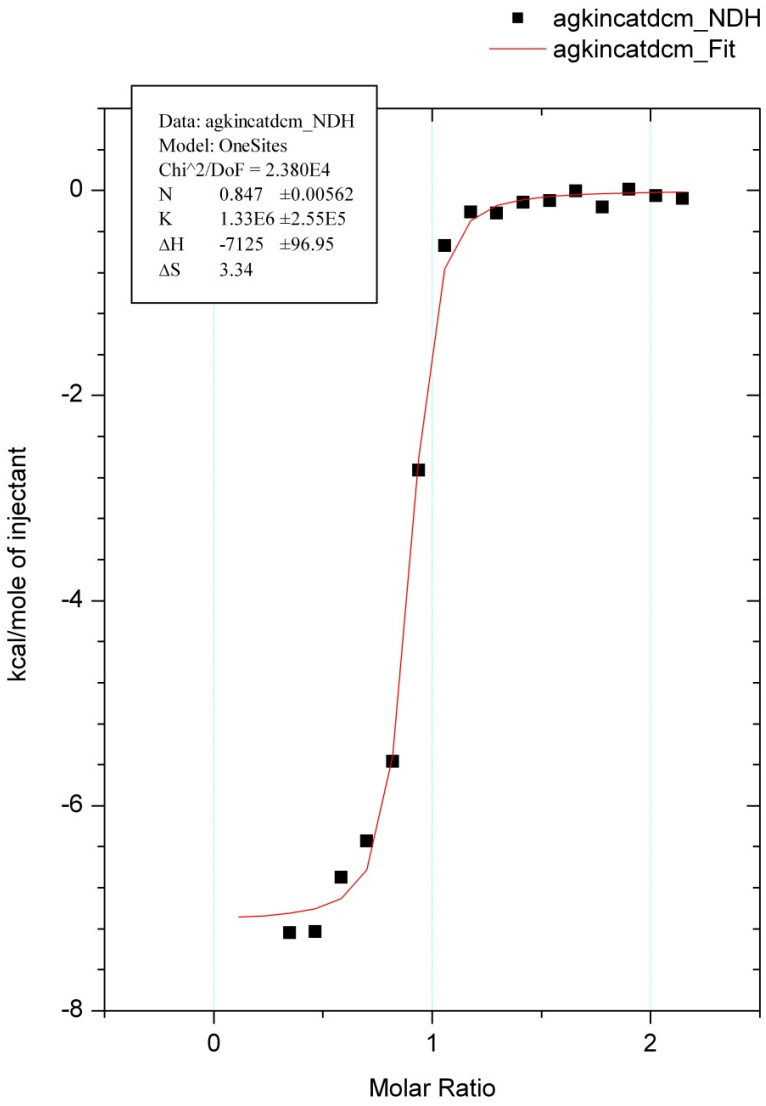

Figure S23. Normalized integration heat *vs* molar ration obtained in the ITC experiment of a CH_2Cl_2 solution of biscatenane **6** with *N*-oxide **7**. Fit to the theoretical binding isotherm (red line) using a 1:1 binding model. The mathematical analysis of the titration data was performed using the Origin software.